XLIII CILAMCE
21–25, November, 2022
FOZ DO IGUAÇU – PR – BRAZIL

Numerical simulation methodology for active-adaptive vibration control using a state-space formulation and IIR filters

Maurizio R. Barghouthi[1], Eduardo L. O. Batista[2], Eduardo M. O. Lopes[1]

[1]*Department of Mechanical Engineering, Federal University of Parana*
Curitiba, 81530-900, Parana, Brazil
maurizio00999@gmail.com, eduardo_lopes@ufpr.br
[2]*Department of Electrical and Electronics Engineering, Federal University of Santa Catarina*
Florianopolis, 88040-900, Santa Catarina, Brazil
eduardo.batista@ufsc.br

Abstract. Undesired vibrations can affect performance, reduce life cycle, and generate excessive noise. Therefore, they should be controlled. The present work focuses on an active-adaptive vibration control approach which is implemented and investigated through simulation and experimental trials. The adaptive feature of the control system allows a satisfactorily low level of vibration to be sustained even if some eventual changes affect the structure of concern. The current control system is composed of sensors, actuators and a control unit with digital filters, in a feedforward architecture that uses the FxNLMS or CVA-FxNLMS adaptive algorithms. Such a system is applied to a clamped-clamped metallic beam subjected to harmonic excitation. The main contribution of this work is the development of a time-domain numerical simulation methodology for the aforementioned system using state-space formulation and IIR filters. The model parameters resulting from such a methodology are adjusted via numerical optimization. The proposed simulation methodology is validated by experimental trials, showing reliable performance.

Keywords: Vibration Control, FxNLMS Algorithm, Adaptive Filter.

1 Introduction

The control of mechanical vibration has many significant applications, for instance, in manufacturing, infrastructure engineering, and consumer products. In this context, unwanted vibrations can affect performance, reduce life cycle, and generate excessive noise. Therefore, such vibrations must be controlled. Vibration control can be defined as a set of techniques that aim to reduce unwanted vibrations that occur in mechanical systems, due to external and/or internal disturbance sources. It is possible to characterize five usual types of vibration control: passive control, semi-active control, active-non adaptive control, active-adaptive control, and hybrid control.

The active-adaptive vibration control strategy consists in generating vibrations that destructively interfere with the vibrations produced by an unwanted disturbance source in a given position of the mechanical system. The analysis process and the design of this type of control architecture are well described by Fuller et al. [1], and recent applications of such architecture can be found in Hansen [2] and Landau et al. [3].

The transient behavior of the control system has attracted attention and then been object of proposal of new adaptive algorithms [4]. In this context, digital emulation is a very convenient tool for studying transient behavior for different types of: (I) disturbances, (II) adaptation steps, (III) penalty factors, and (IV) modal characteristics of mechanical systems, among others.

Several efforts have been made towards obtaining models that emulate the behavior of active-adaptive vibration control systems [5], [6]. The present work is devoted to improving the performance of such models by means of adding the dynamics of subsystems which are not usually represented in the models. More specifically, it is dedicated to the development of a numerical methodology for active-adaptive vibration control using state space formulation and infinite impulse response (IIR) filters. The parameters of the numerical model are obtained by using a numerical optimization approach that considers a frequency function response (FRF) of a experimentally-obtained system path [1][2]. The control action's results are also presented, demonstrating the effectiveness of the numerical model in simulating the experimental reality.

The paper is organized as follows. In section 2, an active-adaptive vibration system's numerical model is developed. Section 3 presents the optimization problem's formulation. Section 4.1 presents the optimization results, while section 4.2 presents the control's numerical/experimental results for different step sizes and algorithms. Finally, section 5 ends the work with the presentation of general conclusions.

2 System path emulation

As a general rule, in active-adaptive vibration control systems, inputs are digitally generated using a hardware platform (e.g., a digital controller), whereas outputs are motion signals at specific points of the mechanical system under control. Between an input and an output, there are several subsystems such as: samplers, interpolators, actuators, mechanical structure and sensors [1]. When these subsystems are organized in a single sequential operation, a system path is defined [1] [2].

The detailed system path diagram considered in this work is illustrated in Fig. 1, which is described by the following sequence: (I) a control unit generates the control signal $c[n]$ with a delay of N_d samples; (II) the signal $c[n - N_d]$ is then sampled and interpolated by the zero-order hold circuit which has the transfer function [7]

$$G_{ho}(s) = \frac{1 - z^{-1}}{s} \tag{1}$$

generating the analog control signal $c(t)$; (III) the signal $c(t)$ feeds the magnetic actuator which excites the mechanical system with a force $f(t)$; (IV) a specific point of the structure moves with an acceleration indicated by $a(t)$. The next sections will describe the discrete-time model of each subsystem in Fig. 1.

Figure 1. System path.

2.1 Emulation of first order linear system

A first order linear system (FOLS) described as

$$\dot{y}(t) = ay(t) + bu(t) \tag{2}$$

with a and b as complex constants, can be easily emulated by a digital computer. Its formulation is carried out by using the impulse response function given by [7]

$$h(t) = be^{at}1(t) \tag{3}$$

where $1(t)$ is the unit step function. It is possible to approximately emulate a continuous-time system $h(t)$ through a discrete system $h[n]$ using the following relationship [7]

$$h[n] = h(n\Delta t)\Delta t. \tag{4}$$

Applying the eq. (4) to eq. (3), one can obtain

$$h(t) = be^{a\Delta tn}\Delta t1[n]. \tag{5}$$

The z transform of the signal defined in eq. (5) is

$$H[z] = b\Delta t(e^{0a\Delta t} + e^{1a\Delta t}z^{-1} + e^{2a\Delta t}z^{-2} + \cdots) \tag{6}$$

For $|z| > \left|e^{a\Delta t}\right|$, it turns out that the above equation is the sum of an infinite geometric progression with a ratio less than 1. Such a summation can be simplified to

$$H[z] = \frac{b\Delta t}{1 - e^{a\Delta t}z^{-1}}. \tag{7}$$

Thus, since eq. (7) corresponds to the discrete model of an IIR filter, one can conclude that the system described in eq. (2) can be digitally emulated according to Fig. 2 [7].

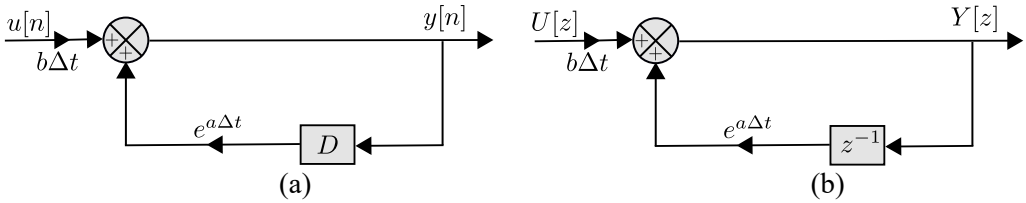

Figure 2. Digital emulation of FOLS: (a) discrete time-domain; (b) z domain.

2.2 Emulation of magnetic actuator

The equivalent circuit for the magnetic actuator considered in this work consists of an inductor with inductance L in series with a resistor with resistance R. Thus, such a circuit can be described by a differential equation in the form [8]

$$\frac{di(t)}{dt} = -\frac{R}{L}i(t) + \frac{1}{L}v(t) \tag{8}$$

where $v(t)$ is the electrical input voltage and $i(t)$ electrical current through the circuit.

For small displacements and considering a linearization near the system operation point, the magnetic force that excites the mechanical system can be considered proportional to the electrical current [9]. Thus,

$$f(t) = K_m i(t). \tag{9}$$

Further, defining the actuator gain as constant and given by $K_{at} = K_m/L$, and the actuator time constant as $\tau_{at} = L/R$, eq. (8) can be rewritten as

$$\frac{df(t)}{dt} = -\frac{1}{\tau_{at}}f(t) + K_{at}v(t). \tag{10}$$

The digital emulation of eq. (10) can then be performed by a FOLS with $a = -1/\tau_{at}$ and $b = K_{at}$ (see Fig. 2).

2.3 Emulation of linear single-degree-of-freedom mechanical systems in the state space

The equation of motion for a linear single-degree-of-freedom mechanical system (LSDOFMS) with mass m, natural frequency ω_n, and damping factor ζ (in which the assumption of viscous damping is implicit) can be written for $q(t)$ as the generalized coordinate, as

$$\ddot{q}(t) + 2\zeta\omega_n\dot{q}(t) + \omega_n^2 q(t) = \frac{1}{m}f(t). \tag{11}$$

This equation can be formulated in state space by [8]

$$\begin{cases} \dot{\mathbf{x}}(t) = \mathbf{A}\mathbf{x}(t) + \mathbf{B}f(t) \\ \mathbf{y}(t) = \mathbf{C}\mathbf{x}(t) + \mathbf{D}f(t) \end{cases} \tag{12}$$

$$\begin{cases} \mathbf{A} = \begin{bmatrix} 0 & 1 \\ -\omega_n^2 & -2\zeta\omega_n \end{bmatrix} \quad \mathbf{B} = \begin{bmatrix} 0 \\ \frac{1}{m} \end{bmatrix} \\ \\ \mathbf{C} = \begin{bmatrix} 1 & 0 \\ 0 & 1 \\ -\omega_n^2 & -2\zeta\omega_n \end{bmatrix} \quad \mathbf{D} = \begin{bmatrix} 0 \\ 0 \\ \frac{1}{m} \end{bmatrix} \end{cases} \tag{13}$$

where the input signal is the force $f(t)$, and the displacement, velocity and acceleration output signals are given by the vector $\mathbf{y}(t) = [q(t)\ \dot{q}(t)\ \ddot{q}(t)]$. The state signals are $\mathbf{x}(t) = [q(t)\ \dot{q}(t)]$.

It is possible to configure the system in diagonal space. To this end, the eigenvalues of matrix $\mathbf{A}$ are calculated through the characteristic equation

$$\Delta = det(\lambda I - A) = \lambda(\lambda + 2\zeta\omega_n) - (-1)(\omega_n^2) = \lambda^2 + 2\zeta\omega_n\lambda + \omega_n^2 \tag{14}$$

whose roots, for $\omega_d = \omega_n\sqrt{1-\zeta^2}$ and $j = \sqrt{-1}$, are

$$\begin{cases} \lambda_1 = -\zeta\omega_n + j\omega_d \\ \lambda_2 = -\zeta\omega_n - j\omega_d. \end{cases} \tag{15}$$

The corresponding eigenvector matrix is

$$\mathbf{P} = \begin{bmatrix} 1 & 1 \\ \lambda_1 & \lambda_2 \end{bmatrix}, \mathbf{P}^{-1} = \frac{1}{-2j\omega_d}\begin{bmatrix} \lambda_2 & -1 \\ -\lambda_1 & 1 \end{bmatrix} \tag{16}$$

Thus, matrix $\mathbf{A}$ can be written as

$$\mathbf{A} = \mathbf{P}\mathbf{\Lambda}\mathbf{P}^{-1} \tag{17}$$

where $\mathbf{\Lambda} = \mathbf{P}^{-1}\mathbf{A}\mathbf{P}$ is the diagonal matrix containing the eigenvalues λ_1 and λ_2.

Defining the coordinate transformation

$$\begin{cases} \mathbf{x}_\lambda(t) = \mathbf{P}^{-1}\mathbf{x}(t) \\ \mathbf{x}(t) = \mathbf{P}\mathbf{x}_\lambda(t). \end{cases} \tag{18}$$

the state equation in the diagonal configuration is

$$\dot{\mathbf{x}}_\lambda(t) = \mathbf{\Lambda}\mathbf{x}_\lambda(t) + \mathbf{P}^{-1}\mathbf{B}\mathbf{f}(t) \tag{19}$$

which consists of 2 decoupled equations in the form

$$\dot{x}_{\lambda.i}(t) = \lambda_i x_{\lambda.i}(t) + f_{\lambda.i}(t) \tag{20}$$

with $i = \{1, 2\}$.

Considering the diagonal configuration described above and recognizing that each eq. (20) corresponds to a FOLS with $a = \lambda_i$, $b = 1$, $u(t) = f_{\lambda.i}(t)$ and $y(t) = x_{\lambda.i}(t)$, it turns out that the mechanical system can be emulated as illustrated in Fig. 3 with the corresponding z transform given by

$$\mathbf{H}_{MCK}[z] = \frac{\mathbf{Y}[z]}{\mathbf{F}[z]} = (\mathbf{C}\mathbf{P}\mathbf{H}_\lambda[z]\mathbf{P}^{-1}\mathbf{B} + \mathbf{D}) \tag{21}$$

where

$$\mathbf{H}_\lambda[z] = \begin{bmatrix} \frac{\Delta t}{1-e^{\lambda_1\Delta t}z^{-1}} & 0 \\ 0 & \frac{\Delta t}{1-e^{\lambda_2\Delta t}z^{-1}} \end{bmatrix}. \tag{22}$$

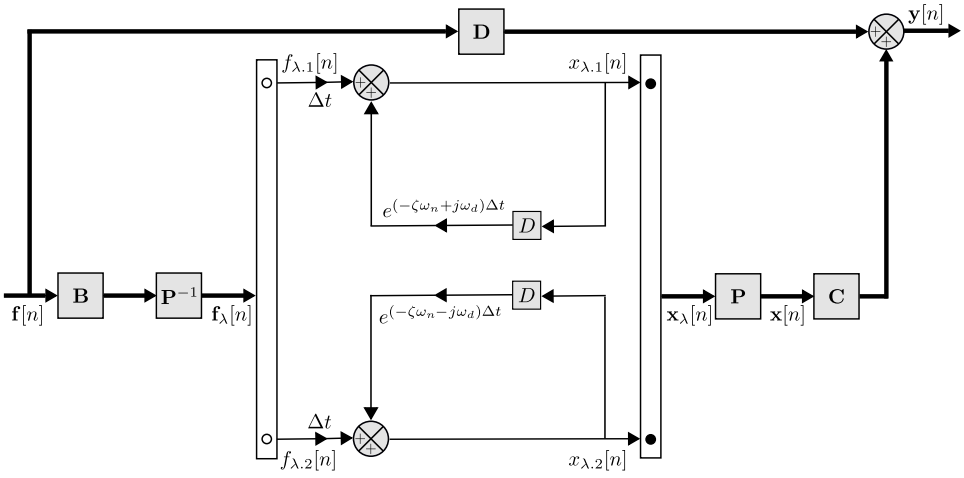

Figure 3. Digital emulation of LSDOFMS.

The emulation architecture for the system in Fig. 3 can be used for any ζ value. It is a more compact form than the architectures developed in [5] and [6], which have a different IIR filter configuration for each type of

system response (i.e, underdamped, critically damped or overdamped). Moreover, one can set up the output of the system in Fig. 3 for the displacement, velocity and acceleration.

The extension to the emulation of Linear Multiple-Degree-of-Freedom Mechanical Systems (LMDOFMS) in modal coordinates can be performed via a linear combination of LSDOFMS as described by Barghouthi et al. [6].

3 Optimization model

Aiming to approximate the FRF $G(z)$ of the proposed numerical model to the experimentally-obtained FRF of the system path, $H(e^{j\Omega})$, an optimization procedure is used in this work. The optimization parameters are the first two natural frequency's (f_{n1}, f_{n2}) and the first two damping factors (ζ_1, ζ_2) of the beam, the delay N_d (see Fig. 1), the magnetic actuator gain K_{at} and magnetic actuator time constant τ_{at}. The optimization parameters are listed in vector $\mathbf{W} = [f_{n1}\ f_{n2}\ \zeta_1\ \zeta_2\ K_{at}\tau_{at}\ N_d]$ and the optimization problem is defined by

$$\begin{aligned} \underset{\mathbf{W}}{\text{minimize}} \quad & \|P(e^{j\Omega}))P^*(e^{j\Omega})\| \\ \text{subject to} \quad & 25 < f_{n1} < 30\ Hz, \\ & 70 < f_{n2} < 80\ Hz, \\ & 0.0001 < \zeta_1 < 0.01, \\ & 0.0001 < \zeta_2 < 0.01, \\ & 0.001 < K_{at} < 1000\ N/AH, \\ & 0.1 < \tau_{at} < 1000\ ms, \\ & 0 < N_d < 10. \end{aligned} \tag{23}$$

where $P(e^{j\Omega}) = G(e^{j\Omega}) - H(e^{j\Omega})$. The intervals for the constraints were chosen around to expected parameter values obtained either via modal analysis [10] or from the electrical characteristics of the system. The constrained sequential quadratic programming method is used to solve the constrained optimization problem [11].

4 Results

In this section, numerical and experimental results are presented. The experimental results were obtained from the following set up: ESP32-WROOM-32 micro-controller operating at a sampling rate of $f_s = 250\ Hz$ (period of 4ms), acceleration sensors LSM6DS3, solenoid electromagnetic actuators, digital-to-analog converter MCP4725 along current buffers based on LM358 amps-ops and TIP41C transistors, analog-to-digital converter ADS1015, and a clamped-clamped ASTM-A36 steel beam, 590 mm long, 40 mm wide and 1.9 mm thick.

The reference sensor was positioned at 130 mm from the top clamp, the error sensor at 460 mm, the control actuator at 160 mm and the disturbance actuator at 430 mm. The distance between the actuators and the beam was 2 mm. Figure 4 presents the experimental set up.

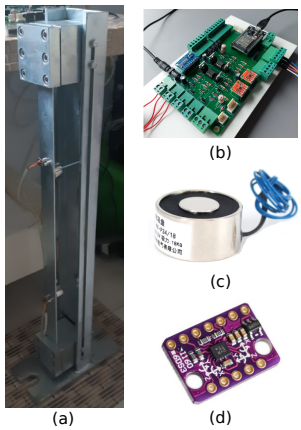

Figure 4. Experimental set up: (a) mechanical structure; (b) control unit; (c) solenoid electromagnet actuator; (d) LSM6DS3 sensor.

4.1 Experiment 1: optimization results

In this first experiment, the focus is to approximate the numerical model $G(e^{j\Omega})$ to the identified feedback path $H(e^{j\Omega})$ [6]. To carry out $H(e^{j\Omega})$ identification, a uniformly distributed white noise voltage signal was applied to the control magnetic actuator and the acceleration captured by the error sensor was recorded. With these signals, an adaptive modeling was performed by using the NLMS algorithm [5]. Then, by applying the Fourier transform to impulse response obtained in such modeling, the function $H(e^{j\Omega})$ results. $\mathbf{W}$ parameters are adjusted so that $H(e^{j\Omega})$ gets close to the numerical model $G(e^{j\Omega})$, according to the optimization problem described in eq. (23).

Optimal parameters of $\mathbf{W}$ were adjusted at $f_{n1} = 28.21\ Hz$, $f_{n2} = 72.41\ Hz$, $\zeta_1 = 0.00169$, $\zeta_2 = 0.00454$, $K_{at} = 17.85\ N/AH$, $\tau_{at} = 7.73\ ms$, and $N_d = 3$. Using a multimeter, the resistance of the solenoids electromagnets actuators was measured at a value of $R = 37\ \Omega$. Therefore, $L = R\tau_{at} = 286\ mH$ and $K_m = K_{at}L = 5.11\ N/A$.

Figure 5 presents the FRFs and the impulse responses of the numerical model and experimentally identified path. It is observed, in general, that the numerical and the experimental curves are in good agreement.

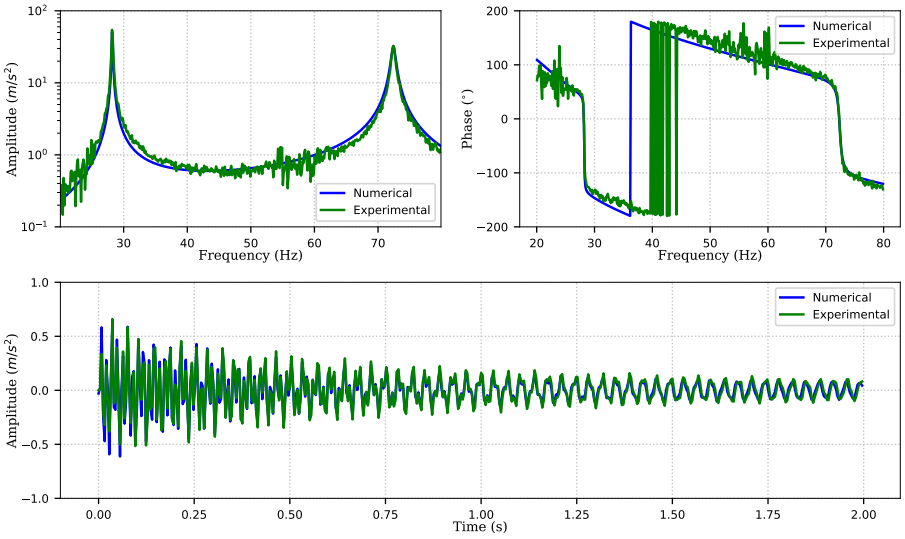

Figure 5. FRFs and impulse responses for the numerical and experimental paths.

4.2 Experiment 2: active control results

The second experiment involves active vibration control using the FxNLMS and CVA-FxNLMS algorithms [4]. In this context, it is considered a harmonic disturbance of 73.2 Hz applied to the beam, with the positioning of sensors and actuators described at the beginning of this section. Such disturbance is applied to the beam until the vibration stabilizes and then the active control is turned on. For convenience, $t = 0$ is defined at that moment. Figures 6 and 7 show, respectively, the normalized mean square error (NMSE) obtained using FxNLMS and CVA-FxNLMS algorithm for different step sizes μ.

The first point to highlight in these results is the similarity between numerical and experimental NMSE waveforms, specially in Fig. 7 (b). Furthermore, the numerical simulation predicts the experimental divergence in Fig. 6 (b). Besides, one can notice that the FxNLMS algorithm has a reduction of 10dB around 1.4 seconds, while in the CVA-FxNLMS algorithm can have the same reduction in 0.5 s. Finally, as expected by Batista et al. [4], the CVA-FxNLMS algorithm can converge with higher adaptation steps, while the FxLMS algorithm has difficulty converging even to small values of μ, which is the case illustrated in the Fig. 6 (b).

5 Conclusion

The present work focuses on the development of a numerical methodology that simulates an active-adaptive vibration control system. A state space formulation was employed, with IIR filters to emulate the system of concern. The adjustment of the physical quantities of the numerical model was carried out via optimization which

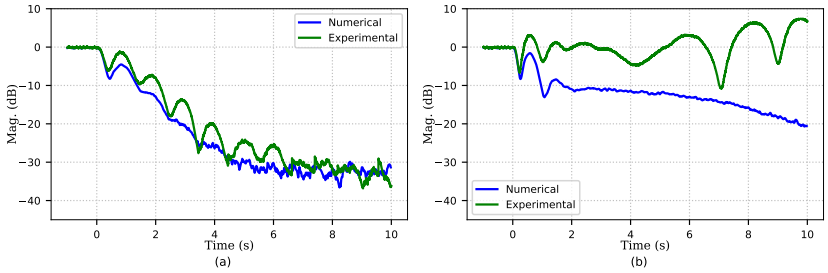

Figure 6. NMSE for active control using the FxNLMS algorithm: (a) $\mu = 0.007$; (b) $\mu = 0.02$.

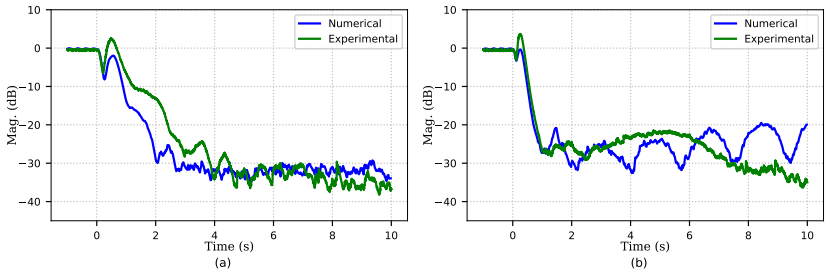

Figure 7. NMSE for active control using the CVA-FxNLMS algorithm: (a) $\mu = 0.02$; (b) $\mu = 0.07$.

seeks to equalize the FRF of the numerical model with the identified experimental path. In general, the obtained results showed very good similarities between simulation and experiment.

Acknowledgements. M.R. Barghouthi and E.M.O Lopes acknowledge the financial support of CAPES (Brazil) and CNPq (Brazil), respectively.

Authorship statement. The authors hereby confirm that they are the sole liable persons responsible for the authorship of this work, and that all material that has been herein included as part of the present paper is either the property (and authorship) of the authors, or has the permission of the owners to be included here.

References

[1] C. R. Fuller, S. J. Elliott, and P. A. Nelson. *Active Control of Vibration*. Academic Press, 1996.
[2] C. Hansen. *Active Control of Noise and Vibration*, volume 1 of *Active Control of Noise and Vibration*. CRC Press, 2013.
[3] I. D. Landau, T.-B. Airimițoaie, A. Castellanos-Silva, and A. Constantinescu. *Adaptive and Robust Active Vibration Control*. Advances in Industrial Control. Springer International Publishing, Cham, 2017.
[4] E. L. O. Batista, M. R. Barghouthi, and E. M. O. Lopes. A novel adaptive scheme to improve the performance of feedforward active vibration control systems. *IEEE/ASME Transactions on Mechatronics*, 2021. DOI: 10.1109/TMECH.2021.3104307.
[5] M. R. Barghouthi, E. L. O. Batista, and E. M. O. Lopes. Numerical and experimental analysis of a hybrid (passive-adaptive) control of vibrations in a cantilever beam under harmonic excitations. In *the Proceedings of the 25th ABCM International Congress of Mechanical Engineering, Uberlândia.*, 2019.
[6] M. R. Barghouthi, E. L. O. Batista, and E. M. O. Lopes. Numerical and experimental analysis of a hybrid (passive-adaptive) vibration control system in a cantilever beam under broadband excitation. In *Vibration Engineering and Technology of Machinery: Proceedings of VETOMAC XV 2019*, pp. 219–232. Springer International Publishing, 2021. DOI: 10.1007/978-3-030-60694-7_14.
[7] K. Ogata. *Discrete-time control systems, 2th Edition*. Prentice Hall Englewood Cliffs, NJ, 1995.
[8] N. S. Nise. *Control Systems Engineering, 7th Edition*. Wiley, 2015.
[9] S. Yadav, S. K. Verma, and S. K. Nagar. Performance enhancement of magnetic levitation system using teaching learning based optimization. *Alexandria Engineering Journal*, vol. 57, n. 4, pp. 2427–2433, 2018.
[10] D. J. Inman. *Engineering Vibrations, International Edition*. Pearson Education Limited, 2013.
[11] S. Rao. *Engineering Optimization: Theory and Practice*. Wiley, 2009.